Featured in Physics

Extreme Violations of Leggett-Garg Inequalities for a System Evolving under Superposition of Unitaries

Arijit Chatterjee,[1,*,†] H. S. Karthik,[2,*,‡] T. S. Mahesh,[1,§] and A. R. Usha Devi[3,‖]
[1]Department of Physics and NMR Research Center, Indian Institute of Science Education and Research, Pune 411008, India
[2]International Centre for Theory of Quantum Technologies, University of Gdansk, 80-308 Gdansk, Poland
[3]Department of Physics, Bangalore University, Bengaluru 560 056, India

(Received 30 January 2025; accepted 30 September 2025; published 24 November 2025)

The violation of Leggett-Garg inequality (LGI) indicates general temporal correlations in quantum systems that cannot be explained classically. Under unitary dynamics and projective measurements, the violation of LGI is restricted up to the temporal Tsirelson's bound (TTB). Here, we consider superposition of unitary time evolutions and find them to produce an enhancement in the violation of LGI beyond the TTB, growing monotonically with increasing superposition. We experimentally realize superposition of unitaries in NMR systems and demonstrate this enhanced violation. In the presence of noise, such superposition of unitaries remarkably extend the time of LGI violation, showcasing improved robustness against decoherence. This opens up possibilities of employing such nontrivial dynamical maps for robust quantum control, along with provoking research on characterizing correlations in general sequential measurement scenarios.

DOI: 10.1103/vydp-9qqq

Introduction—The twilight zone between classical and quantum worlds [1–3] has been under perpetual investigation since the dawn of quantum mechanics [4–6]. Quantum physics radically differs from its classical counterpart primarily due to the postulates of state description and measurement. For single systems, a possible construction of a classical world view adheres to the notion of "macrorealism" [7–9], which says that a system, capable of being in two or more distinct states, will always be in any one of them, and it is possible to determine this state with arbitrarily small perturbation on the subsequent dynamics. In [7], Leggett and Garg considered measuring two-point correlations $C_{ij} = \langle q(t_i)q(t_j)\rangle$ in a system, where $q(t_k)$ is the outcome of a dichotomous (± 1 valued) observable $\hat{Q}$ at time t_k, and $\langle\cdot\rangle$ means an average over multiple runs of the experiment. They found, for any choice of times t_1, t_2, and t_3, the assumptions of macrorealism restrict the value of a particular linear combination of two-point correlators $K_3 = C_{12} + C_{23} - C_{13}$ as $-3 \leq K_3 \leq 1$, which is known as Leggett-Garg inequality (LGI). However, quantum systems can defy macrorealism by surpassing the upper bound (classical) of LGI. Thus, violation of LGI acts as a certification of nonclassicality and it has been observed experimentally in a variety of quantum systems [10–13].

Early experimental [10,11] and theoretical studies [14,15] suggest that for a qubit, evolving under unitary dynamics, the maximum violation of LGI is constrained by the temporal Tsirelson bound (TTB), which reads $(K_3)_{\mathrm{m}} \leq 1.5$, where $(K_3)_{\mathrm{m}}$ denotes the maximum value of K_3. This shows that even quantum theory restricts $(K_3)_{\mathrm{m}}$ way below its algebraic maximum value 3. However, recently, it was shown that it is possible to observe the violation of LGI beyond the TTB either by replacing the qubit with a multilevel system [16–18] or by replacing unitary evolution with a non-Hermitian $\mathcal{PT}$ symmetric evolution on a qubit [19–22].

The superposition of states allows a quantum system to exhibit nonmacrorealistic behavior by violating LGI up to the TTB. This provokes us to consider superposition of unitary time evolutions and ask what happens to the violation of LGI for a qubit undergoing such a transformation. We construct unitary transformations by doing superposition of time evolution unitaries. Subjecting a qubit under such superposition of unitaries, we find clear violation of LGI beyond the TTB, growing with the strength of superposition. We obtain a way of physically realizing these superposed unitaries using an ancillary system and experimentally demonstrate the enhanced nonmacrorealism using nuclear magnetic resonance (NMR) techniques. As an application, we report robustness in the behavior of a qubit when it is subjected to such a transformation. At longer times, due to the presence of environmental noise, qubits get decohered [1,2,23,24] and the LGI violation disappears, indicating the emergence of classicality [11,13]. However, our superposed unitaries provide robustness against such environmental

*These authors contributed equally to this work.
†Contact author: arijitchattopadhyay01@gmail.com
‡Contact author: hsk1729@gmail.com
§Contact author: tsmahesh@gmail.com
‖Contact author: ushadevi@bub.ernet.in

 © 2025 American Physical Society

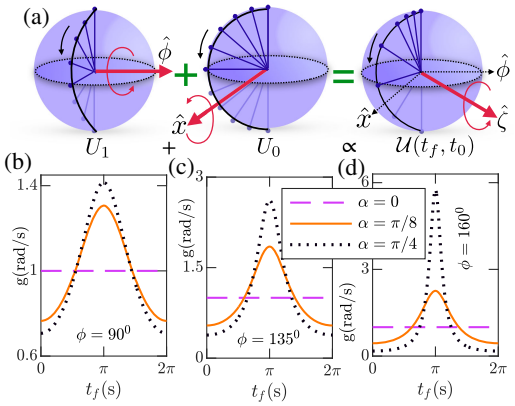


FIG. 1. (a) Superposition of two unitaries U_0 and U_1 (for $\phi = \pi/2$) on the Bloch sphere shifts the rotation axis (thick arrow) and introduces nonlinearities in SOE (modeled by the gap in the spokes). (b)–(d) SOE for the initial state $|0\rangle$ against final time t_f for different values of α and ϕ at $\omega = 1$.

noise by remarkably increasing the time to which LGI violation persists.

Superposition of unitaries—Consider two unitary transformations $U_0 = \exp(-i\sigma_x\omega[t_f - t_0]/2)$ and $U_1 = \exp(-i\sigma_\phi\omega[t_f - t_0]/2)$, which transform the state of a qubit from time t_0 to t_f. σ_k denotes the Pauli matrix along $\hat{k}$, and $\hat{\phi}$ is an axis making an angle ϕ with $\hat{x}$ [see Fig. 1(a)]. U_0 and U_1 describe rotations of the Bloch vector about $\hat{x}$ and $\hat{\phi}$, respectively. We construct an effective unitary transformation by superposing them as

$$\mathcal{U}(t_f, t_0) \coloneqq (\cos\alpha U_0 + \sin\alpha U_1)/\mathcal{N}(t_f, t_0), \quad (1)$$

$$\text{and} \quad \mathcal{N}^2(t_f, t_0) \coloneqq \text{tr}\left[\tilde{\mathcal{U}}_+^\dagger(t_f, t_0)\tilde{\mathcal{U}}_+(t_f, t_0)\right]/2, \quad (2)$$

with $\tilde{\mathcal{U}}_\pm(t_f, t_0) = \cos\alpha U_0 \pm \sin\alpha U_1$, where α is the superposition parameter with no superposition for $\alpha = 0, \pi/2$ and maximum superposition at $\alpha = \pi/4$. On the other hand, ϕ is the angle between the rotation axis of U_0 and U_1, thereby indicating how "distinct" the unitaries are that are being superposed. The superposed unitary is well defined as long as $\mathcal{N}^2(t_f, t_0) > 0$, and we restrict $\alpha \in [0, \pi/2]$ and $\phi \in [0, \pi)$ to ensure the same for all t_0 and t_f. A general method for constructing such effective unitary transformation beyond qubits is presented in Supplemental Material [25].

To understand the action of $\mathcal{U}(t_f, t_0)$ on a random state $|\psi_0\rangle$, we fix t_0 and continuously increase t_f so that $|\psi_{t_f}\rangle = \mathcal{U}(t_f, t_0)|\psi_0\rangle$ traces a continuous trajectory $(\theta(t_f), \Phi(t_f))$ on the surface of the Bloch sphere. Here $\theta(t_f)$ and $\Phi(t_f)$ are the colatitude and longitude of the Bloch vector at time t_f. We define the speed of evolution (SOE) of the Bloch vector as $\vec{g}(t_f) \coloneqq \partial_{t_f}(\theta(t_f), \Phi(t_f))$. For simplicity, we choose $|\psi_0\rangle = |0\rangle$, the eigenstate of σ_z with the eigenvalue 1, which gets transformed as $|\psi_{t_f}\rangle = \cos[f(t_f)/2]|0\rangle - i\sin[f(t_f)/2]\exp(i\zeta)|1\rangle$, where $f(t)$ and ζ depend on α and ϕ. The SOE is now reduced to just one component $g(t_f) = \partial_{t_f} f(t_f)$, which is a nonlinear function of t_f. Therefore, the superposed unitary $\mathcal{U}(t_f, t_0)$ effectively describes a rotation of the Bloch vector with nonlinear SOE, with a shift in the axis of rotation $\hat{\zeta}$ [see Fig. 1(a)]. As shown in Figs. 1(b)–1(d), the nonlinearity of SOE increases with increasing superposition α. Also, at a α, the SOE gets more nonlinear as we make U_0 and U_1 increasingly distinct by rising ϕ. (see Appendix A).

Note that, as $\mathcal{U}(t_f, t_0)$ depends nonlinearly on $(t_f - t_0)$, the product law does not follow: $\mathcal{U}(t_3, t_1) \neq \mathcal{U}(t_3, t_2)\,\mathcal{U}(t_2, t_1)$. Thus, it does not describe closed system evolution. Therefore, to realize $\mathcal{U}(t_f, t_0)$, we consider the conditional evolution of the system qubit (S), depending on the state of an ancillary qubit (A) [26,27]. Under an interaction unitary $\mathcal{V}_{AS} = |0\rangle\langle 0| \otimes U_0 + |1\rangle\langle 1| \otimes U_1$, S evolves under U_0 or U_1, conditioned on whether A is in state $|0\rangle$ or $|1\rangle$, respectively. Therefore, to realize a superposition between U_0 and U_1, we initialize A in the state $|\alpha\rangle_A = \cos\alpha|0\rangle + \sin\alpha|1\rangle$, let it interact with S from t_0 to t_f under $\mathcal{V}_{AS}$, and finally postselect A in state $|+\rangle = (|0\rangle + |1\rangle)/\sqrt{2}$ [see Fig. 2(a)], such that S gets transformed under the $\mathcal{U}(t_f, t_0)$ (see Supplemental Material [25] for details). The circuit of Fig. 2(a) thus serves as a physical realization of the superposed unitary for any quantum simulator. Linear combination of unitaries like $\mathcal{U}(t_f, t_0)$ (generally nonunitary) has also been explored in other contexts [28–32].

LGI for a qubit under superposed unitary $\mathcal{U}$—Choosing the initial state $\rho_{t_0} = \mathbb{1}/2$, C_{ij} for dichotomous observable

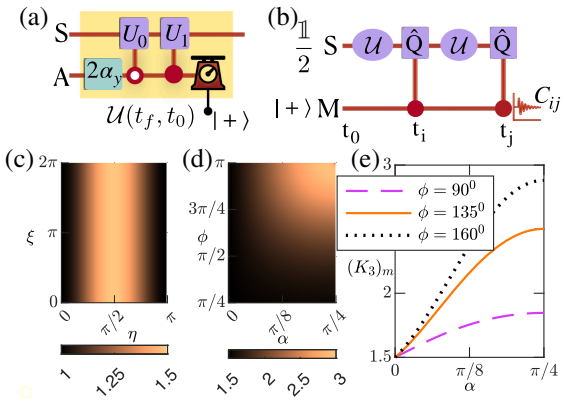


FIG. 2. (a) A quantum circuit for realizing the superposed unitary using an ancillary qubit (A), which, after interacting with S, gets postselected in state $|+\rangle$. (b) The interferometric circuit to determine C_{ij} corresponding to observable $\hat{Q}$ using an additional qubit M. (c) $(K_3)_m$ against the longitude (ξ) and the colatitude (η) of $\hat{k}$, confirming the TTB under simple unitaries. (d) $(K_3)_m$ vs α and ϕ showing violation of the TTB under superposed unitaries. (e) $(K_3)_m$ vs α for different ϕ values showing violation of the TTB explicitly.

$\hat{Q}$ can be measured using the interferometric circuit [33] shown in Fig. 2(b). Here the correlation between measurement outcomes of $\hat{Q}$ is stored in the phase of an additional qubit (M) initiated in state $|+\rangle_{\mathrm{M}}$. The measurement of M's coherence $\mathcal{C} := [\langle\hat{\sigma}_x\rangle + i\langle\hat{\sigma}_y\rangle]/2$ directly gives C_{ij} as

$$\mathrm{Re}[\mathcal{C}] = \frac{1}{2}\mathrm{tr}\left[\hat{Q}\mathcal{U}(t_j,t_i)\hat{Q}\mathcal{U}^{\dagger}(t_j,t_i)\right] = C_{ij}. \tag{3}$$

We set $t_0 = t_1 = 0, t_2 = t$, and $t_3 = 2t$ to determine $C_{12}(t)$, $C_{23}(t)$, and $C_{13}(t)$ for $\hat{Q} = \hat{\sigma}_z$. First, we let S (with initial state $\mathbb{1}/2$) to evolve under the simple unitary (no superposition) $U = \exp(-i\omega\sigma_k t)$ and note the maximum of $K_3(t)$ over $t \in [0, 2\pi]/\omega$ as $(K_3)_{\mathrm{m}}$, which is plotted for each possible $\hat{k}$ in Fig. 2(c) confirming the existence of the TTB as $(K_3)_{\mathrm{m}} \leq 1.5$. Next, we subject S (with the same initial state) under the superposed unitary and again plot $(K_3)_{\mathrm{m}}$ as a function of α and ϕ in Fig. 2(d), which shows increase of $(K_3)_{\mathrm{m}}$ beyond the TTB with increasing α. This enhanced violation beyond the TTB with rising α is plotted explicitly in Fig. 2(e) for $\phi = 90°, 135°$, and $160°$. These results clearly show that, for any given ϕ, the superposition of unitary produces enhanced violation of LGI which increases with increasing superposition. Moreover, this violation increases with ϕ for a fixed α and K_3 approaches its algebraic maximum $(K_3)_{\mathrm{m}} = 3$ at $\alpha = \pi/4$ as $\phi \to \pi$.

Experiments—We choose the three spin-1/2 nuclei of ^{13}C-dibromofluoromethane (DBFM) molecule as our three-qubit quantum register [see Fig. 3(a)], identifying ^{13}C as S, ^{19}F as A, and ^{1}H as M. In a strong magnetic field of 11.7 T (along $\hat{z}$), the liquid ensemble of DBFM, dissolved in acetone-d6, rests in thermal equilibrium at an ambient temperature of 300 K. Under high temperature–high field assumption [34], the density matrix of the quantum register reads $\rho_{\mathrm{th}} = \mathbb{1}/8 + \epsilon(\gamma_{\mathrm{C}} I_z^{\mathrm{S}} + \gamma_{\mathrm{F}} I_z^{\mathrm{A}} + \gamma_{\mathrm{H}} I_z^{\mathrm{M}})$, where γ_i is the gyromagnetic ratio of the i th nucleus, $I_z^v := \hat{\sigma}_z^v/2$, and the purity factor $\epsilon \approx 10^{-5}$. In a triply rotating frame, rotating at the resonant frequency of each nucleus, the Hamiltonian of the quantum register reads [34,35] $\mathcal{H}_{\mathrm{NMR}} = 2\pi(J_{\mathrm{SA}} I_z^{\mathrm{S}} I_z^{\mathrm{A}} + J_{\mathrm{SM}} I_z^{\mathrm{S}} I_z^{\mathrm{M}} + J_{\mathrm{AM}} I_z^{\mathrm{A}} I_z^{\mathrm{M}})$.

We first initialize the quantum register into the pseudo-pure state $\rho_{\mathrm{in}} = (\mathbb{1}/2)_{\mathrm{S}} \otimes |0+\rangle\langle 0+|_{\mathrm{AM}}$ [36–38], after which, the quantum circuit of Fig. 3(b) is used to perform the experiments, where we combine the circuit of Fig. 2(a) with the interferometric circuit of Fig. 2(b). Measuring the real part of the coherence $\mathcal{C}_{\mathrm{M}}$ at the end of the circuit gives

$$\mathrm{Re}[\mathcal{C}_{\mathrm{M}}] = \frac{1}{4}(T_+(t_j,t_i) + T_-(t_j,t_i))$$
$$\text{where } T_{\pm}(t_j,t_i) = \mathrm{tr}\left[\hat{\sigma}_z\tilde{\mathcal{U}}_{\pm}(t_j,t_i)\hat{\sigma}_z\frac{\mathbb{1}}{2}\tilde{\mathcal{U}}_{\pm}^{\dagger}(t_j,t_i)\right]. \tag{4}$$

The terms $T_+(t_j,t_i)$ and $T_-(t_j,t_i)$ can be measured separately via distinct spectral lines in NMR, which is equivalent to postselecting A in $\{|+\rangle, |-\rangle\}$ basis (see Appendix C). Just switching off two controlled $\hat{\sigma}_z$ gates, an identical run of the quantum circuit of Fig. 3(b) gives the measurement outcome $\mathrm{Re}[\mathcal{C}_{\mathrm{M}}] = (\mathcal{N}^2(t_j,t_i) + \tilde{\mathcal{N}}^2(t_j,t_i))/4$, with $\mathcal{N}^2(t_j,t_i)$ as defined in Eq. (2) and $\tilde{\mathcal{N}}^2(t_j,t_i) = \mathrm{tr}[\mathcal{U}_-^{\dagger}(t_j,t_i)\mathcal{U}_-(t_j,t_i)]/2$. $\mathcal{N}^2(t_j,t_i)$ and $\tilde{\mathcal{N}}^2(t_j,t_i)$ can again be measured separately as before. It can be easily seen from Eqs. (1) and (3) that $C_{ij} = T_+(t_j,t_i)/\mathcal{N}^2(t_j,t_i)$. This allows direct experimental measurement of C_{ij} by setting appropriate t_i and t_j. Note that our method allows us to choose any value of the α and ϕ.

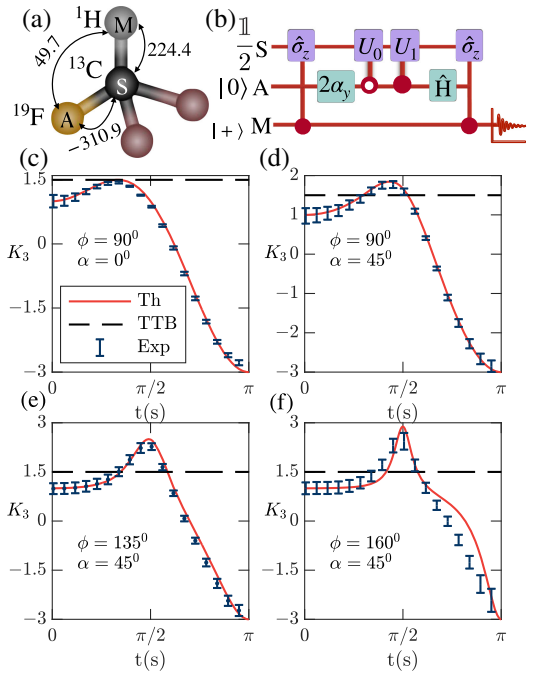


FIG. 3. (a) The molecular structure of DBFM with respective J_{ij} values in hertz. (b) Quantum circuit for determining C_{ij} ($\hat{\mathrm{H}}$ is the Hadamard gate). (c)–(f) Experimentally measured values of K_3 vs theoretical curves (solid curves) for different values of α and ϕ. Error bars account for systematic (rf inhomogeneity) and random errors (thermal noise).

As in the theory, we set $t_1 = 0, t_2 = t, t_3 = 2t$, and $\omega = 1$ for our experiments. For no superposition, we set $\alpha = 0$ and measure K_3 while increasing t from 0 to π. Results are shown in Fig. 3(c), confirming the existence of the TTB as expected. Next, we consider the maximum superposition $\alpha = \pi/4$ at $\phi = \pi/2$ and measure K_3 with increasing t and observe a clear violation beyond the TTB [see Fig. 3(d)]. We increase ϕ to 135° and 160° at maximum superposition of $\alpha = \pi/4$ and measure K_3 with varying t. We observe enhanced violation beyond the TTB with increasing ϕ, as predicted theoretically. Experimentally measured value of $(K_3)_{\mathrm{m}}$ reads 2.27 ± 0.1 for $\phi = 135°$, showing enhanced violation by more than 7 times the experimental uncertainty [Fig. 3(e)], and 2.43 ± 0.25 for

$\phi = 160°$, which violates LGI beyond the TTB by more than 3 times the experimental uncertainty [Fig. 3(f)]. These results clearly and convincingly demonstrate the enhanced violation of LGI beyond the TTB due to superposition of unitaries.

Enhanced robustness—We now investigate the effect of dephasing on the dynamics under the superposed unitary. In Eq. (3), the observable $\hat{Q}(0) = \hat{\sigma}_z$ is subjected under $\mathcal{U}(t,0)$ to get transformed to $\hat{Q}(t) = \mathcal{U}^\dagger(t,0)\hat{\sigma}_z\mathcal{U}(t,0)$. Upon increasing t continuously from 0, this map describes rotation of the Bloch vector $\hat{z}$ (representing the observable) about $\hat{\zeta}$ with nonlinear SOE $g(t)$ [see Eq. (A6) in Appendix A]. Writing the observable at time t as $\hat{Q}(t) = \vec{S}(t)\cdot\vec{\sigma}$, with Bloch vector $\vec{S}(t) \coloneqq (S_x(t), S_y(t), S_z(t))$ and Pauli vector $\vec{\sigma} \coloneqq (\hat{\sigma}_x, \hat{\sigma}_y, \hat{\sigma}_z)$, the rotation is described by the Bloch equation [34,39], where dephasing can be phenomenologically introduced with decay rate γ as

$$\partial_t \vec{S}(t) = g(t)\hat{\zeta}\times\vec{S}(t) - \gamma\Big(\hat{z}\times[\vec{S}(t)\times\hat{z}]\Big). \tag{5}$$

Equation (5) is solved with initial condition $\vec{S}(0) = (0,0,1)$ to get $\vec{S}(t)$ and $\vec{S}(2t)$, from which we directly compute $K_3(t) = \hat{z}\cdot[2\vec{S}(t) - \vec{S}(2t)]$ (see Appendix B). The quantum lifetime of the system τ_α is defined as the time up to which LGI violation persists under $\mathcal{U}$ at superposition α. The gain in lifetime due to superposition is plotted against α for different values of ϕ in Fig. 4(a), which depicts the remarkable enhancement of robustness against dephasing with increasing superposition. However, in practice, $\mathcal{U}(t,0)$ is realized via an ancillary system (A) as shown in Fig. 2(a), where S evolves jointly with A until postselection. Therefore, we apply the dephasing noise to both S and A, and compute the gain in lifetime as before (see Appendix D for details). Results are plotted for different values of ϕ in Fig. 4(b), which shows that even the presence of additional noise in A does not destroy the robustness achieved by the superposition of unitaries against dephasing.

Role of SOE—From Eq. (3), it can be directly seen that [see Eq. (B1) in Appendix B] for $\hat{Q} = \hat{\sigma}_z$, $C_{ij} = \mathcal{U}^\dagger(t_j,t_i)[\hat{z}]\cdot\hat{z}$, where $\hat{z}$ is the initial Bloch vector at time t_i, representing the observable, and $\mathcal{U}^\dagger(t_j,t_i)[\hat{z}]$ is the Bloch vector at t_j corresponding to the transformed observable under the action of $\mathcal{U}(t_j,t_i)$. At zero superposition, $\mathcal{U}(t_j,t_i)$ describes rotation at frequency ω about $\hat{x}$ (or $\hat{\phi}$). Therefore, for our choice of $t_0 = t_1 = 0, t_2 = t$, and $t_3 = 2t$, if it rotates $\hat{z}$ by an angle ωt in time t, the rotation in time $2t$ will be $2\omega t$, resulting $K_3 = 2\cos(\omega t) - \cos(2\omega t)$, which always remains upper bounded by 1.5. This shows that the TTB originates from the linearity of rotation of the Bloch vector and necessitates a nonlinear SOE for violation beyond the TTB. As an example, for K_3 to approach its algebraic maximum 3, we need C_{12} and C_{13} to approach 1 and -1, respectively, at the same value of t. This requires $\mathcal{U}^\dagger$ to rotate the vector $\hat{z}$ almost none in 0 to t but by an angle π from t to $2t$, which can only be performed with extreme nonlinear SOE. As shown in Figs. 1(b)–1(d), the act of superposition causes the SOE to get increasingly nonlinear with increasing α for each value of ϕ, which correspondingly results in enhanced violation of the TTB with increasing α. Figures 1(b)–1(d) show that, at a given α, the nonlinearity in SOE increases with increasing ϕ, which explains the increasing violation beyond the TTB in Figs. 3(e) and 3(f).

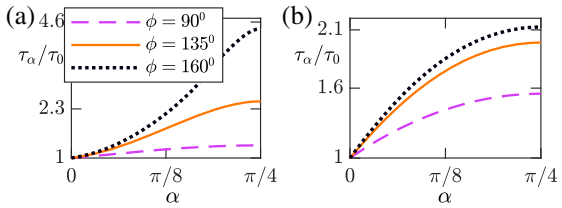


FIG. 4. The gain in lifetime τ_α/τ_0 (τ_0 being lifetime at $\alpha = 0$) vs α at different values of ϕ calculated from (a) Eq. (5) and (b) from applying noise on both S and A. In both cases, decay constant $\gamma = 1/(4\pi)$ s^{-1}.

Conclusions—We investigated temporal correlations in terms of LGI for qubit transforming under a superposition of unitaries. We found temporal correlations get stronger and violate LGI beyond the TTB under such superposed unitaries. This enhanced nonmacrorealism, as quantified by the violation of LGI beyond the TTB, increases with increasing superposition between the unitaries. Also, at a given superposition, it increases as we make the angle between the axis of rotation larger between two unitaries that are being superposed. We present a method to physically realize the superposition of unitaries using an ancillary qubit and experimentally verify the enhanced nonmacrorealism in NMR architecture. Moreover, we found that the dynamics under the superposed unitary have applications in providing more robustness against environmental noise by remarkably enhancing the time up to which the system violates LGI under decoherence. We believe that our Letter will pave the way for further investigations on applying these superposed unitaries in various quantum information processing tasks like [40], along with provoking foundational questions on the nature of temporal correlations in quantum systems in interaction with other ancillary system.

Acknowledgments—A. C. acknowledges Vishal Varma for useful suggestions regarding software setting of the plots. H. S. K. thanks NCN Poland, ChistEra-2023/05/Y/ST2/00005 under the project Modern Device Independent Cryptography (MoDIC). T. S. M. acknowledges funding from DST/ICPS/QuST/2019/Q67 and I-HUB Quantum Technology Foundation. A. R. U. is funded by DST/ICPS/QuST/2019/Q107.

Data availability—The data that support the findings of this article are openly available [41].

[1] W. H. Zurek, Decoherence, einselection, and the quantum origins of the classical, Rev. Mod. Phys. **75**, 715 (2003).

[2] W. H. Zurek, Preferred states, predictability, classicality and the environment-induced decoherence, Prog. Theor. Phys. **89**, 281 (1993).

[3] W. H. Zurek, Quantum Darwinism, classical reality, and the randomness of quantum jumps, Phys. Today **67**, No. 10, 44 (2014).

[4] A. Einstein, B. Podolsky, and N. Rosen, Can quantum-mechanical description of physical reality be considered complete?, Phys. Rev. **47**, 777 (1935).

[5] J. S. Bell, On the Einstein Podolsky Rosen paradox, Phys. Phys. Fiz. **1**, 195 (1964).

[6] R. P. Feynman and F. L. Vernon, Jr., The theory of a general quantum system interacting with a linear dissipative system, Ann. Phys. (N.Y.) **281**, 547 (2000).

[7] A. J. Leggett and A. Garg, Quantum mechanics versus macroscopic realism: Is the flux there when nobody looks?, Phys. Rev. Lett. **54**, 857 (1985).

[8] A. J. Leggett, Realism and the physical world, Rep. Prog. Phys. **71**, 022001 (2008).

[9] Y. Zhang, X. Tan, and T. Qiu, Comparing various formulations of macrorealism, Quantum Inf. Process. **22**, 354 (2023).

[10] A. Palacios-Laloy, F. Mallet, F. Nguyen, P. Bertet, D. Vion, D. Esteve, and A. N. Korotkov, Experimental violation of a Bell's inequality in time with weak measurement, Nat. Phys. **6**, 442 (2010).

[11] V. Athalye, S. S. Roy, and T. S. Mahesh, Investigation of the Leggett-Garg inequality for precessing nuclear spins, Phys. Rev. Lett. **107**, 130402 (2011).

[12] H. Katiyar, A. Shukla, K. R. K. Rao, and T. S. Mahesh, Violation of entropic Leggett-Garg inequality in nuclear spins, Phys. Rev. A **87**, 052102 (2013).

[13] G. Waldherr, P. Neumann, S. F. Huelga, F. Jelezko, and J. Wrachtrup, Violation of a temporal Bell inequality for single spins in a diamond defect center, Phys. Rev. Lett. **107**, 090401 (2011).

[14] C. Budroni, T. Moroder, M. Kleinmann, and O. Gühne, Bounding temporal quantum correlations, Phys. Rev. Lett. **111**, 020403 (2013).

[15] T. Fritz, Quantum correlations in the temporal Clauser–Horne–Shimony–Holt (CHSH) scenario, New J. Phys. **12**, 083055 (2010).

[16] C. Budroni and C. Emary, Temporal quantum correlations and Leggett-Garg inequalities in multilevel systems, Phys. Rev. Lett. **113**, 050401 (2014).

[17] K. Wang, C. Emary, X. Zhan, Z. Bian, J. Li, and P. Xue, Enhanced violations of Leggett-Garg inequalities in an experimental three-level system, Opt. Express **25**, 31462 (2017).

[18] H. Katiyar, A. Brodutch, D. Lu, and R. Laflamme, Experimental violation of the Leggett–Garg inequality in a three-level system, New J. Phys. **19**, 023033 (2017).

[19] H. S. Karthik, H. Akshata Shenoy, and A. R. U. Devi, Leggett-Garg inequalities and temporal correlations for a qubit under *PT*-symmetric dynamics, Phys. Rev. A **103**, 032420 (2021).

[20] A. V. Varma, J. E. Muldoon, S. Paul, Y. N. Joglekar, and S. Das, Extreme violation of the Leggett-Garg inequality in nonunitary dynamics with complex energies, Phys. Rev. A **108**, 032202 (2023).

[21] P. Lu, X. Rao, T. Liu, Y. Liu, J. Bian, F. Zhu, and L. Luo, Experimental demonstration of enhanced violations of Leggett-Garg inequalities in a *PT*-symmetric trapped-ion qubit, Phys. Rev. A **109**, 042205 (2024).

[22] C.-W. Wu, M.-C. Zhang, Y.-L. Zhou, T. Chen, R. Huang, Y. Xie, B.-Q. Ou, W. Wu, A. Miranowicz, J. Zhang *et al.*, Observation of quantum temporal correlations well beyond Lüders bound, Phys. Rev. Res. **7**, 013058 (2025).

[23] K. Hornberger, Introduction to decoherence theory, in *Entanglement and Decoherence: Foundations and Modern Trends* (Springer, New York, 2009), pp. 221–276.

[24] E. Joos, H. D. Zeh, C. Kiefer, D. J. Giulini, J. Kupsch, and I.-O. Stamatescu, *Decoherence and the Appearance of a Classical World in Quantum Theory* (Springer Science & Business Media, Berlin, Heidelberh, 2013).

[25] See Supplemental Material at http://link.aps.org/supplemental/10.1103/vydp-9qqq for generalizations beyond qubits and beyond three-terms LGI, along with computational and experimental details.

[26] S. S. Roy, A. Shukla, and T. S. Mahesh, NMR implementation of a quantum delayed-choice experiment, Phys. Rev. A **85**, 022109 (2012).

[27] K. Goswami, C. Giarmatzi, M. Kewming, F. Costa, C. Branciard, J. Romero, and A. G. White, Indefinite causal order in a quantum switch, Phys. Rev. Lett. **121**, 090503 (2018).

[28] L. Gui-Lu, General quantum interference principle and duality computer, Commun. Theor. Phys. **45**, 825 (2006).

[29] L. Gui-Lu and L. Yang, Duality computing in quantum computers, Commun. Theor. Phys. **50**, 1303 (2008).

[30] L. Gui-Lu, L. Yang, and W. Chuan, Allowable generalized quantum gates, Commun. Theor. Phys. **51**, 65 (2009).

[31] S. Gudder, Mathematical theory of duality quantum computers, Quantum Inf. Process. **6**, 37 (2007).

[32] Y. Zhang, H. Cao, and L. Li, Realization of allowable generalized quantum gates, Sci. China Phys. Mech. Astron. **53**, 1878 (2010).

[33] O. Moussa, C. A. Ryan, D. G. Cory, and R. Laflamme, Testing contextuality on quantum ensembles with one clean qubit, Phys. Rev. Lett. **104**, 160501 (2010).

[34] J. Cavanagh, *Protein NMR Spectroscopy: Principles and Practice* (Academic Press, New York, 1996).

[35] M. H. Levitt, *Spin Dynamics: Basics of Nuclear Magnetic Resonance* (John Wiley & Sons, New York, 2008).

[36] D. G. Cory, A. F. Fahmy, and T. F. Havel, Ensemble quantum computing by NMR spectroscopy, Proc. Natl. Acad. Sci. U.S.A. **94**, 1634 (1997).

[37] N. A. Gershenfeld and I. L. Chuang, Bulk spin-resonance quantum computation, Science **275**, 350 (1997).

[38] D. G. Cory, M. D. Price, and T. F. Havel, Nuclear magnetic resonance spectroscopy: An experimentally accessible paradigm for quantum computing, Physica (Amsterdam) **120D**, 82 (1998).

[39] J. D. Roberts, The Bloch equations. How to have fun calculating what happens in NMR experiments with a personal computer, Concepts Magn. Reson. **3**, 27 (1991).

[40] F. J. Gómez-Ruiz, J. J. Mendoza-Arenas, F. J. Rodríguez, C. Tejedor, and L. Quiroga, Quantum phase transitions detected by a local probe using time correlations and violations of Leggett-Garg inequalities, Phys. Rev. B **93**, 035441 (2016).
[41] A. Chatterjee, H. S. Karthik, T. S. Mahesh, and A. R. Usha Devi, Superposition of unitaries, GitHub, 2025, https://github.com/QBoyArijit/Superposition_of_Unitaries/tree/main.
[42] D. A. Lidar, Lecture notes on the theory of open quantum systems, arXiv:1902.00967.
[43] H.-P. Breuer and F. Petruccione, *The Theory of Open Quantum Systems* (Oxford University Press, USA, 2002).

End Matter

Appendix A: Properties of the superposed unitaries and defining the SOE—We take two arbitrary directions $\hat{n} = n_x\hat{x} + n_y\hat{y} + n_z\hat{z}$ and $\hat{m} = m_x\hat{x} + m_y\hat{y} + m_z\hat{z}$ in the Bloch sphere and construct a superposition between $U_0(t_f, t_0) = \exp(-\mathrm{i}\hat{\sigma}_n\omega\delta/2)$ and $U_1(t_f, t_0) = \exp(-\mathrm{i}\hat{\sigma}_m\omega\delta/2)$ according to Eq. (1) of main text to form $\mathcal{U}(t_f, t_0)$, where $\delta = t_f - t_0$. The unnormalized operator reads

$$\begin{aligned}\tilde{\mathcal{U}}_+(t_f,t_0) &= \cos(\alpha)U_0(t_f,t_0) + \sin(\alpha)U_1(t_f,t_0)\\ &= (\cos(\alpha)+\sin(\alpha))\cos\frac{\omega\delta}{2}\mathbb{1}\\ &\quad - \mathrm{i}(\cos(\alpha)\hat{\sigma}_n + \sin(\alpha)\hat{\sigma}_m)\sin\frac{\omega\delta}{2}. \end{aligned} \tag{A1}$$

Using this, we find

$$\begin{aligned}&\tilde{\mathcal{U}}_+(t_f,t_0)\tilde{\mathcal{U}}_+^\dagger(t_f,t_0)\\ &= \underbrace{\left[1+\sin(2\alpha)\left(\cos^2\frac{\omega\delta}{2} + \hat{n}\cdot\hat{m}\sin^2\frac{\omega\delta}{2}\right)\right]}_{\mathcal{N}^2(t_f,t_0)}\mathbb{1}, \end{aligned} \tag{A2}$$

which ensures that the superposed operator $\mathcal{U}(t_f, t_0) = \tilde{\mathcal{U}}(t_f, t_0)/\mathcal{N}(t_f, t_0)$ is always an unitary operator for arbitrary values of t_f and t_0 and for arbitrary choices of directions $\hat{n}, \hat{m}$, as long as $-1 < \hat{n}\cdot\hat{m} \le 1$, which is required to ensure the positivity of $\mathcal{N}^2(t_f, t_0)$ for all values of t_0, t_f and $\alpha \in [0, \pi/4]$ [see Supplemental Material [25] Eq. (6)].

Without loss of generality, we consider $\hat{n} := \hat{x}$ and $\hat{m} := \hat{\phi}$ as in the main text, where $\hat{\phi}$ is a unit vector making an angle $\phi \in [0, \pi)$ with $\hat{x}$. Taking $t_0 = 0$ and $t_f = t$, the superposed unitary can be expanded as

$$\begin{aligned}\mathcal{U}(t,0) &= \frac{\begin{bmatrix}(\cos\alpha+\sin\alpha)\cos\frac{\omega t}{2} & -\mathrm{i}(\cos\alpha+\mathrm{e}^{-\mathrm{i}\phi}\sin\alpha)\sin\frac{\omega t}{2}\\ -\mathrm{i}(\cos\alpha+\mathrm{e}^{\mathrm{i}\phi}\sin\alpha)\sin\frac{\omega t}{2} & (\cos\alpha+\sin\alpha)\cos\frac{\omega t}{2}\end{bmatrix}}{\sqrt{1+\sin(2\alpha)\left[\cos^2\frac{\omega t}{2}+\cos\phi\sin^2\frac{\omega t}{2}\right]}} = \underbrace{\frac{(\cos\alpha+\sin\alpha)\cos\frac{\omega t}{2}}{\sqrt{1+\sin(2\alpha)\left[\cos^2\frac{\omega t}{2}+\cos\phi\sin^2\frac{\omega t}{2}\right]}}}_{\cos[f(t)/2]}\mathbb{1}\\ &\quad - \mathrm{i}\underbrace{\frac{\sqrt{1+\cos\phi\sin(2\alpha)}\sin\frac{\omega t}{2}}{\sqrt{1+\sin(2\alpha)\left[\cos^2\frac{\omega t}{2}+\cos\phi\sin^2\frac{\omega t}{2}\right]}}}_{\sin[f(t)/2]}\left(\underbrace{\frac{\cos\alpha+\cos\phi\sin\alpha}{\sqrt{1+\cos\phi\sin(2\alpha)}}}_{\cos\zeta}\hat{\sigma}_x + \underbrace{\frac{\sin\alpha\sin\phi}{\sqrt{1+\cos\phi\sin(2\alpha)}}}_{\sin\zeta}\hat{\sigma}_y\right)\\ &= \cos\left[\frac{f(t)}{2}\right]\mathbb{1} - \mathrm{i}\sin\left[\frac{f(t)}{2}\right]\hat{\sigma}_\zeta, \end{aligned}$$

where $\hat{\sigma}_\zeta := \cos\zeta\hat{\sigma}_x + \sin\zeta\hat{\sigma}_y$. To define the SOE $g(t)$, we take the initial state $|\psi_0\rangle := |0\rangle$ and let it transform under the superposed unitary as

$$|\psi_t\rangle = \mathcal{U}(t,0)|0\rangle = \cos\left[\frac{f(t)}{2}\right]|0\rangle - \mathrm{i}\sin\left[\frac{f(t)}{2}\right]\mathrm{e}^{\mathrm{i}\zeta}|1\rangle = \cos\left[\frac{f(t)}{2}\right]|0\rangle + \sin\left[\frac{f(t)}{2}\right]\mathrm{e}^{\mathrm{i}(\zeta-\pi/2)}|1\rangle. \tag{A3}$$

Therefore, if we increase t continuously from 0, Eq. (A3) describes counterclockwise rotation of the Bloch vector $\hat{z}$ about axis $\hat{\zeta} \coloneqq \cos\zeta\hat{x} + \sin\zeta\hat{y}$ in the Bloch sphere. SOE $[g(t)]$ can now be defined as the rate of change of the colatitude (which is the only degree of freedom that is changing here) of the Bloch vector with t as

$$g(t) = \partial_t f(t) = \frac{-2\partial_t \cos[f(t)/2]}{\sin[f(t)/2]}. \tag{A4}$$

Computing the derivatives, we get

$$\partial_t \cos[f(t)] = -\frac{\omega(1+\sin(2\alpha)\cos\phi)(\cos\alpha+\sin\alpha)\sin\frac{\omega t}{2}}{2\left[1+\sin(2\alpha)\left(\cos^2\frac{\omega t}{2}+\cos\phi\sin^2\frac{\omega t}{2}\right)\right]^{3/2}}, \tag{A5}$$

which directly gives a closed form expression for the SOE as

$$g(t) = \frac{\omega\sqrt{1+\cos\phi\sin(2\alpha)}(\cos\alpha+\sin\alpha)}{1+\sin(2\alpha)\left(\cos^2\frac{\omega t}{2}+\cos\phi\sin^2\frac{\omega t}{2}\right)}. \tag{A6}$$

Of course, SOE can be defined more generally by taking a generic initial state as $|\psi_0\rangle$ instead of $|0\rangle$. In that case, both the colatitude and longitude of the Bloch vector will change with t, and therefore $g(t)$ will read as the magnitude of the vector sum of these two rate of changes. However, the special case presented here suffices for the requirements of this Letter.

Appendix B: The observable evolution in the Heisenberg picture—One can unravel Eq. (3) by considering the Bloch vector $\vec{S}(0)$ (in our case $\hat{z}$) corresponding to the observable $\hat{Q}$ at time t_i, where $\hat{Q} = \vec{S}(t_i)\cdot\vec{\sigma}$. In the Heisenberg picture, under the action of superposed unitary $\mathcal{U}(t_j,t_i)$, this Bloch vector gets rotated to $\vec{S}(t_j) = \mathcal{U}^\dagger[\hat{z}]$, where $\mathcal{U}^\dagger(t_j,t_i)\hat{Q}\mathcal{U}(t_j,t_i) = \vec{S}(t_j)\cdot\vec{\sigma}$. From Eq. (3), the correlator can now be rewritten as

$$\begin{aligned} C_{ij} &= \frac{1}{2}\mathrm{tr}[\mathcal{U}^\dagger(t_j,t_i)\sigma_z\mathcal{U}(t_j,t_i)\sigma_z] \\ &= \frac{1}{2}\mathrm{tr}[(\mathcal{U}^\dagger[\hat{z}]\cdot\vec{\sigma})\sigma_z] = \mathcal{U}^\dagger[\hat{z}]\cdot\hat{z} = \vec{S}(t_j)\cdot\vec{S}(t_i). \end{aligned} \tag{B1}$$

Appendix C: Experimental details—Here we first derive Eq. (4) of the main text. Evolution of the quantum register under the quantum circuit shown in Fig. 3(b) in the main text reads

$$\begin{aligned}
&\frac{1}{2}(|0\rangle\langle 0| + |1\rangle\langle 1| + |0\rangle\langle 1| + |1\rangle\langle 0|)_{\mathrm{M}} \otimes [\cos^2(\alpha)|0\rangle\langle 0| + \sin^2(\alpha)|1\rangle\langle 1| + \cos(\alpha)\sin(\alpha)(|0\rangle\langle 1| + |1\rangle\langle 0|)]_{\mathrm{A}} \\
&\otimes \left(\frac{\mathbb{1}}{2}\right)_{\mathrm{S}}\downarrow(|0\rangle\langle 0|_{\mathrm{M}} \otimes \mathbb{1}_{\mathrm{S}} + |1\rangle\langle 1|_{\mathrm{M}} \otimes (\sigma_z)_{\mathrm{S}}) \\
&\qquad \frac{1}{2}\left(|0\rangle\langle 0|_{\mathrm{M}} \otimes \left[\frac{\mathbb{1}}{2}\right]_{\mathrm{S}} + |1\rangle\langle 1|_{\mathrm{M}} \otimes \left[\frac{\mathbb{1}}{2}\right]_{\mathrm{S}}\right)(|0\rangle\langle 1|_{\mathrm{M}} + |1\rangle\langle 0|_{\mathrm{M}}) \\
&\otimes \left[\frac{\sigma_z}{2}\right]_{\mathrm{S}}\Bigg) \otimes (.)_{\mathrm{A}}\downarrow(U_0 \otimes |0\rangle\langle 0| + U_1 \otimes |1\rangle\langle 1|)_{\mathrm{AS}} \\
&\qquad\qquad \frac{1}{2}\Bigg(\ldots + |1\rangle\langle 0|_{\mathrm{M}} \otimes \Bigg(\cos^2(\alpha)|0\rangle\langle 0|_{\mathrm{A}} \otimes \left[U_0\frac{\sigma_z}{2}U_0^\dagger\right]_{\mathrm{S}} \\
&+ \sin^2(\alpha)|1\rangle\langle 1|_{\mathrm{A}} \otimes \left[U_1\frac{\sigma_z}{2}U_1^\dagger\right]_{\mathrm{S}} + \cos(\alpha)\sin(\alpha)|0\rangle\langle 1|_{\mathrm{A}} \otimes \left[U_0\frac{\sigma_z}{2}U_1^\dagger\right]_{\mathrm{S}} \\
&+ |1\rangle\langle 0|_{\mathrm{A}} \otimes \left[U_1\frac{\sigma_z}{2}U_0^\dagger\right]_{\mathrm{S}}\Bigg)\downarrow(|0\rangle\langle 0|_{\mathrm{M}} \otimes \mathbb{1}_{\mathrm{S}} + |1\rangle\langle 1|_{\mathrm{M}} \otimes (\sigma_z)_{\mathrm{S}}) \\
&\frac{1}{2}\Bigg(\ldots + |1\rangle\langle 0|_{\mathrm{M}} \otimes \Bigg(\cos^2(\alpha)|0\rangle\langle 0|_{\mathrm{A}} \otimes \left[\sigma_z U_0\frac{\sigma_z}{2}U_0^\dagger\right]_{\mathrm{S}} + \sin^2(\alpha)|1\rangle\langle 1|_{\mathrm{A}} \otimes \left[\sigma_z U_1\frac{\sigma_z}{2}U_1^\dagger\right]_{\mathrm{S}} \\
&+ \cos(\alpha)\sin(\alpha)|0\rangle\langle 1|_{\mathrm{A}} \otimes \left[\sigma_z U_0\frac{\sigma_z}{2}U_1^\dagger\right]_{\mathrm{S}} + |1\rangle\langle 0|_{\mathrm{A}} \otimes \left[\sigma_z U_1\frac{\sigma_z}{2}U_0^\dagger\right]_{\mathrm{S}}\Bigg)\downarrow\hat{\mathrm{H}}_{\mathrm{A}} \to \mathrm{tr}_{\mathrm{AS}}[.]
\end{aligned}$$

$$\rho_{\mathrm{M}} = \frac{1}{2}|+\rangle\langle +|(T_+ + T_-), \tag{C1}$$

which results the (real) NMR signal $S = \mathrm{tr}[\sigma_x \rho_M] = \frac{1}{4}(T_+ + T_-)$ when M is measured. This completes the derivation of Eq. (4) in the main text. Just following these line of steps, the similar results for $\mathcal{N}$ of the main text can also be derived directly.

Finally, note that, during NMR signal acquisition, the final three-qubit state effectively evolves under $\mathcal{H}_{\mathrm{NMR}}$ of the main text. This causes the T_+ and T_- of Eq. (C1) to evolve at different frequencies. Therefore, by taking a Fourier transform of the time domain signal, we go to the frequency domain where we find T_+ and T_- as separate spectral lines. This allows us to postselect the $T_\pm$ terms, which is equivalent to postselecting A in $\{|+\rangle, |-\rangle\}$ basis.

Appendix D: Robustness against dephasing—As mentioned in the main text, for a practical realization of the superposed unitary $\mathcal{U}$, the system S and the ancilla A would both undergo noisy evolutions. To consider this aspect, we subject the joint state ρ_{AS} under a Gorini-Kossakowski-Sudarshan-Lindblad master equation [42,43]

$$\partial_t \rho_{\mathrm{AS}} = -\mathrm{i}[\mathcal{H}_{\mathrm{AS}}, \rho_{\mathrm{AS}}] + \frac{\gamma}{2} \sum_{j=\mathrm{S,A}} (\hat{\sigma}_z^j \rho_{\mathrm{AS}} \hat{\sigma}_z^j - \rho_{\mathrm{AS}}), \quad \text{(D1)}$$

where $\hat{\sigma}_z^j$ denotes the action of $\hat{\sigma}_z$ on j and identity on the rest, and the interaction Hamiltonian reads $\mathcal{H}_{\mathrm{AS}} \coloneqq |0\rangle\langle 0| \otimes \omega\hat{\sigma}_x/2 + |1\rangle\langle 1| \otimes \omega\hat{\sigma}_\phi/2$. In presence of noise ($\gamma > 0$), the initial joint state $\rho_{\mathrm{AS}}(0) = |\alpha_{\mathrm{A}}\rangle\langle\alpha \mathrm{A}| \otimes \mathbb{1}_{\mathrm{S}}/2$ evolves under Eq. (D1) from $t = 0$ to t. After which, A is postselected in state $|+\rangle_{\mathrm{A}}$, allowing S to transform under the map $\mathcal{W}(t, 0)$. The map $\mathcal{W}(t, 0)$ describes the effective dynamics under superposed unitary and dephasing and reads $\mathcal{W}(t, 0)\rho_{\mathrm{S}} = \mathrm{tr}_{\mathrm{A}}[|+\rangle\langle+|_{\mathrm{A}} \exp(\mathcal{L}t)\rho_{\mathrm{AS}}(0)]/\mathrm{tr}[|+\rangle\langle+|_{\mathrm{A}} \exp(\mathcal{L}t)\rho_{\mathrm{AS}}(0)]$, considering the Liouvillian for Eq. (D1) as $\mathcal{L}$. The correlators C_{12}, C_{23}, and C_{13} are computed as before with $\mathcal{W}$ replacing $\mathcal{U}$ in Eq. (3) of the main text. From this, we compute $K_3(t)$ to find the gain in lifetime τ_α/τ_0 with increasing α.

Appendix E: On the enhancement of LGI beyond the TTB—We highlight here the need to involve a higher-dimensional space in order to realize the effective evolution [Eq. (1) in the main text] on the system leading to enhanced violation of the LGI. In a heuristic way, this violation beyond the TTB is reflected via the SOE of the observable (under the superposition of unitaries). Essentially, the act of projecting the ancilla on to a maximal coherent state $[(|0\rangle + |1\rangle)/\sqrt{2}]$ results in a nonlinearity in the SOE, which manifests as the violation of LGI surpassing the TTB. Thus, involving an ancilla and embedding the system qubit into a two-qubit Hilbert space is necessary for realizing violations beyond the TTB. This stands well in agreement with the discussions presented in [19,20].